OBSERVATIONS ON THE ENERGY RESOLUTION OF GERMANIUM DETECTORS FOR 0.1—10 MeV GAMMA RAYS*

H. M. Mann, H. R. Bilger,** and I. S. Sherman

Argonne National Laboratory
Argonne, Illinois

SUMMARY

The ratio of variance to yield was studied for γ-rays at energies up to 10.080 MeV in lithium-drifted germanium detectors. With detectors of thickness up to 14 mm this ratio was found to be as low as 0.13 ± 0.02 at 122 and 356 keV. At energies between 1 and 10 MeV the ratio was found to be 0.16 ± 0.01, corresponding to a detector contribution of 4.8 ± 0.1 keV (FWHM) at 10 MeV. Investigation of the dependence of the ratio of variance to yield on electric field intensity resulted in acceptance of $F = 0.13 \pm 0.02$ as the best experimental estimate of the Fano factor, and $F = 0.16$ is interpreted as an upper limit for γ-rays at energies between 1 and 10 MeV.

INTRODUCTION

The Fano factor F is defined by equation (1):

$$\overline{(N - \overline{N})^2} = \overline{(\triangle N)^2} = F \cdot \overline{N} \qquad (1)$$

where $\overline{N}$ = average number of electron-hole pairs, or yield

$\overline{(N - \overline{N})^2}$ = variance .

The quantity F is a parameter which is restricted to the generation process and should not be used to include additional line-broadening effects.

With detectors of capacitance less than 10 pf and reverse current less than 100 pA, and with the availability of low-noise charge-sensitive preamplifiers (i.e., equivalent noise less than 2 keV (FWHM) for germanium detectors), meaningful investigation of the Fano factor is possible at low energy.[1] The present measurements were carried out with γ-rays at energies of 122 keV and 356 keV, and at various energies from 980 keV to 10.080 MeV.

Earlier experimental estimates of F are given in Table I. The discrepancy between these two values exceeds the assigned standard errors. In contrast with these estimates we have previously shown[4,5] on the basis of a detector contribution of 1.9 keV (FWHM) that

$$F \leq 0.2 \text{ at } E_\gamma = 1.33 \text{ MeV} .$$

These results suggest that there are sources of systematic error in the various attempts to determine F which are not yet fully identified.

In this work[6,7] we confined our measurements to those systems for which electronic noise and drift did not exceed 900 eV (FWHM) at energies below 1 MeV, and was less than 2 keV (FWHM) at 1.33 MeV. In measurements at 6 - 10 MeV, only those detectors for which the detector contribution at 1.33 MeV did not exceed 1.9 keV were used.

THEORETICAL CONSIDERATIONS

In order to evaluate the ratio of variance to yield for the generation process, which we call the intrinsic Fano-factor,[7] we have to consider other line-broadening effects such as the following:

a) electronic noise of the detector-preamplifier system, which may be the

* Work performed under the auspices of the U. S. Atomic Energy Commission.

** On leave from Oklahoma State University.

dominant source of broadening at low energies.

b) drift, i.e. gain instability of the amplifier - analyzer system (including, e.g., instability of bias-levels, etc.)

c) broadening due to high counting rate

d) recombination; i.e., the statistics of recombination

e) trapping; i.e., the statistics of trapping

f) risetime; i.e., the statistics of the collection time of the pairs generated.

We examined reasonable models for these effects and found that in all cases, if they are not properly accounted for, the experimental estimate of the intrinsic Fano-factor will always be too large. Effects d), e), and f) will in general depend on the electric field in the detector in a systematic manner. A variation of the detector voltage will also affect effect a) through variations of detector capacitance and detector reverse current.

The evaluation procedure was such that if both pulser-lines and γ-lines appear as Gaussians in a least-squares fit, we feel justified in subtracting quadratically the pulser width from the γ-line-width in order to obtain the net width due to the intrinsic Fano factor and fluctuations in charge collection.

If we assume a linear recombination of the electron-hole pairs and a diffusion length of the carriers which is large in comparison with the dimensions of the detector, we obtain for the average number of recombining electron-hole pairs[7]

$$\Delta\overline{N}_{Rec} \simeq \overline{N}_o \frac{d}{\mu \cdot \tau \cdot E} = \frac{\alpha}{E} \qquad (2)$$

$\overline{N}_o$ = average number of generated pairs

d = thickness of detector

$\mu \cdot \tau \cdot E$ = "Schubweg".

Assuming a Poisson-distribution of the number of recombining pairs,

$$\sigma^2 = \overline{(\Delta N_{Rec} - \Delta\overline{N}_{Rec})^2} = \overline{\Delta N}_{Rec} = \frac{\alpha}{E}. \qquad (3)$$

These equations suggest a plot of the peak shift versus the reciprocal field strength and a plot of the variance vs the reciprocal field-strength. Further, from the results of equation (2) the slope in equation (3) can be calculated and compared with measurements.

EXPERIMENTAL EQUIPMENT

Detectors

The detectors were prepared by diffusion of lithium into germanium at a temperature of 400 - 450° C for approximately 15 min, followed by a period of up to 10 - 12 weeks for the lithium-drift preparation of a compensated thickness of up to 14 mm. Shorter time intervals were required for compensation of the thinner detectors. The thicknesses of the various detectors used ranged from 3 to 14 mm. They were planar with either circular or rectangular areas of from 0.5 to 8 cm^2. The detectors were mounted in a chamber such as the one shown in Fig. 1,[8] and operated at liquid nitrogen temperature.

Vacuum Tube Amplifier

The vacuum tube preamplifier is characterized by a noise slope of 0.04 keV/pf and a noise intercept of 1.65 ± 0.1 keV, as observed with 2 - 1 μsec integrating time constants after the preamplifier. It consists of three sections and is shown schematically in Fig. 2. The first section, with two E810F (7788) tubes in cascode contains a charge-sensitive amplifier which provides an output voltage pulse of $\frac{Q\ (coulomb)}{2.5 \times 10^{-12}\ (farads)}$ where Q is the charge deposited within the detector. This section is followed by a voltage amplifier with a gain of 200. The third section is an output stage with a voltage gain of 2. This stage will drive a 91-ohm terminated line. The overall sensitivity of the preamplifier is 3 volts/MeV. The rise time is approximately 0.1 msec and the decay time 1 μsec.

Figs. 3 and 4 show the layout of components for the input stage and for the entire preamplifier, respectively. All components used in the input stage were cleaned and checked for electrical leakage prior to assembly, and recleaned after assembly if necessary. The behavior of the E810F(7788) made it necessary to sweep the plate voltage of V_1 through a range of approximately 25 volts below the normal operating value. This was done by use of a shorting switch in the control grid circuit of V_2 (See Fig. 2). For those tubes which exhibited marginal noise behavior (i.e., 1.8 - 2.0 keV (FWHM) for germanium detectors) an adjustment of the current through V_1 and V_2 was used to reduce the noise to the desired value. This was done by replacement of the 3010 Ω resistor in the plate circuit of V_1. Final checkout of the preamplifier included presetting the adjustable 100 KΩ resistor in this circuit and further adjustment of this resistor was not necessary until V_1 or V_2 were replaced. Failure or deterioration of V_1 or V_2 was no problem, however, and the preselection and tube operating conditions

have led to satisfactory performance of the input stage for as long as two years in more than 12 such preamplifiers. Other components such as resistors and capacitors in the input stage are prone to failure, especially at voltages in excess of 1200 V for the detector.

A linear amplifier such as the Ortec 203, or a similar one manufactured by IDP, was used. Several commercial analyzers were employed in the measurements and the experimental data were recorded either in typewritten form or on IBM cards to facilitate plotting and computation. Calibration pulses were obtained from either a mercury-wetted-contact pulse generator or a diode-chopper pulse generator such as the Berkeley Nucleonics Company RP-1.

Transistor Preamplifier[9]

The first stage is mounted inside the chamber and consists of a DC-coupled field-effect transistor (FET). The FET is connected by means of a feed-through to a bipolar transistor in a cascode arrangement, followed by a high-gain preamplifier in an operational feedback loop. Filtering and post-amplification is done with a Tennelec-TC-200 amplifier. We achieved a noise-equivalent of 0.57 keV (FWHM) for germanium with zero added capacitance and an increase of 37 eV per pf.

MEASUREMENTS

$E_\gamma \leq 2.614$ MeV

In this energy range the measurements were made with both vacuum tube preamplifiers and FET-amplifier systems. In Fig. 5 a plot of the peak shift of a ^{133}Ba γ-ray at 356 keV vs 1/E is shown. In Fig. 6 we show results of measurements of the square of FWHM vs 1/E (after subtraction of the electronic noise). Typically, the electronic noise contribution was between 0.8 keV and 0.9 keV FWHM. Similar measurements were made at 122 keV (^{57}Co). Fig. 7 shows a biased spectrum of ^{60}Co, where the electronic pulse-width is 1.5 keV, and the 1.17 MeV and 1.33 MeV-lines have FWHM of 2.4 keV (the 1.17 MeV-line appears smaller due to non-linearities of the system). In Figure 8 and 9 the field-strength - dependence of peak-shift and - width is presented.

In Fig. 10 we show a typical measurement used to determine the branching ratio for the 993 keV γ-ray in the decay of ^{43}K.[4] Calibration runs, such as the one shown in Fig. 7, were used for determination of stability and energy calibration of the system. In these measurements the energy scale corresponded to 0.5 or 0.6 keV/channel and the actual value was determined to ± 0.3 keV by means of voltage measurements.

A radium-thorium source was used for the measurements at an energy of 2614 keV. This energy is associated with ^{208}Tl, commonly known as ThC". Some of these measurements were recorded in a 400 channel analyzer for which it was necessary to preset the pulse generator to a known pulse height on an energy scale corresponding to 1 keV/channel and then expand to 0.5 keV/channel by adjustment of amplifier gain. A typical measurement at this energy is shown in Fig. 11. Although some evidence of low-energy tailing appears for this energy in this particular detector, the mean pulse height and the percent tailing were not affected for a 50% reduction in detector bias below the value used in this measurement.

$6 \leq E_\gamma \leq 10$ MeV

When gamma rays produced in (n, γ) reactions with Cd or Mg as a target, are used for measurements the observed energy is reduced by 511 or 1022 keV below that of the gamma ray since we are looking at peaks associated with the escape of one of both annihilation quanta from the detector. A typical experimental run is shown in Fig. 12. The total line width for these peaks corresponds to 5.6 keV (FWHM) or less, and electronic pulse-widths of not less than 2.5 keV (FWHM), usually 3.0 keV or higher, were frequently recorded. Although this particular run was not used, it presents clear evidence of an energy resolving capability of the detector less than that previously demonstrated.

Measurements were made at these energies with the aid of a variable repetition rate pulse generator that allowed for adequate determination of effects of instability in the amplifier system, and a 1000 channel analyzer. During these measurements the causes of instability were not brought completely under control, and the electronic width including drift was close to 5 keV (FWHM) for periods of 2 1/2 hours or more. Some illustrative data are shown in Fig. 13.

ANALYSIS OF THE DATA

A least squares computation was used for each run to determine the values for the variance σ_γ^2 and σ_p^2 for the gamma-ray line and for the pulse generator, respectively. All runs where a drift of 1 channel or more occurred, except those at energies about 6 MeV, were rejected. For energies above 6 MeV a composite of 5 - 2 1/2 hour runs was used in order to minimize the effect of long-term drift, typically 0.5 keV per hour. A summary of the measurements is shown in Fig. 14, and the higher energy results are tabulated in Table II. A least squares fit of these higher energy data resulted in $F = 0.16 \pm 0.01$. The measurements at 122 keV and 356 keV result in a field-

independent ratio of variance-to-yield and $F = 0.13 \pm 0.02$. Other measurements at 1.333 and 2614 keV gave a dependence of the observed ratio of variance to yield on the electric field intensity, as shown in Fig. 16. A similar effect was observed at higher energies.

DISCUSSION

Figures 5 and 8 show the observations of peak shift as a function of field-strength. With equations (1) and (2) the slope of $\frac{\sigma^2}{N}$ vs $\frac{1}{E}$ can be calculated. In both cases this contribution should be negligible. Figure 6 shows no discernible field-strength dependence of the FWHM. However, the Co^{60} - results (Fig. 9) indicate a field-dependence of FWHM, as do the results in Fig. 15.

Since equation (3) gives the dependence of FWHM solely on the basis of Poisson-distributed recombination we conclude that in many of our measurements above 1 MeV other processes lead to a field-dependent FWHM. However one should bear in mind, that any theory of the field-dependence has to be compatible with the observations of relatively small peak shifts versus field-strength. Our intention is in subsequent experiments to determine the time behavior of the FWHM in order to get information about trapping processes.

At present we cannot exclude the possibility of drift in the amplifying system. However, as long as such processes lead to a gaussian distribution of pulser- and γ-lines we would expect to obtain the net distribution of the collected pairs by quadratic subtraction. On the other hand, if there is drift at a constant rate during the accumulation, which leads to addition of "drift width" to electronic width, as well as drift width to γ-width, then the quadratic subtraction always leads to too high a value for the estimate of F.

CONCLUSION

We conclude that the intrinsic Fano-factor for γ-rays (or electrons) in germanium at liquid nitrogen temperature (78° K) is

$F = 0.13 \pm 0.02$ at 122 and 356 keV

$F \leq 0.16 \pm 0.01$ at 1 MeV $\leq E \leq$ 10 MeV .

ACKNOWLEDGMENT

The detector preparation was carried out largely by H. W. Helenberg and F. J. Janarek. Valuable assistance was provided by R. M. Kliss, J. G. Semmelman and R. W. Westholm. The data in Fig. 9 were supplied by R. Smither. H. E. Jackson and G. E. Thomas generously relinquished their experimental set-up at the reactor CP-5 for some of these measurements. We are grateful for the interest and encouragement of L. M. Bollinger.

REFERENCES

[1] H. R. Bilger and I. S. Sherman, Phys. Lett., to be published.

[2] G. T. Ewan and A. J. Tavendale, Can. J. Phys. 42, 2286-2331 (November, 1964).

[3] Sven O. W. Antman, Donald A. Landis and Richard H. Pehl, UCRL-16317 (Sept. 24, 1965).

[4] R. E. Holland, F. J. Lynch, and H. M. Mann Bull. Am. Phys. Soc. 10, 119 (1965).

[5] H. M. Mann, IEEE Trans. Nucl. Sci. 12, 88 (1965).

[6] H. M. Mann, Bull. Am. Phys. Soc. 11, 127 (1966).

[7] H. R. Bilger and H. M. Mann, Bull. Am. Phys. Soc. 11, 127 (1966).

[8] C. E. Miner, "Mountings and housings for Lithium-drifted Silicon and Germanium-detectors", UCRL-11946 (Feb. 24th, 1965).

[9] I.S. Sherman, Argonne National Laboratory, to be published.

TABLE I

Previous Experimental Estimates of the Fano Factor for Germanium

$F_{exptl.}$	Energy	Reference
0.45 ± 0.045	122 to 2614 keV	2
0.30 ± 0.03	122 to 2614 keV	3

TABLE II

Detector Contribution to Total Resolution Width

Energy Deposited In Detector (keV)	No. of Determinations	$\triangle E$ (keV)
898.2 (^{88}Y)	5	1.50 ± 0.05
1063.5 (^{207}Bi)	3	1.66 ± 0.08
1332.5 (^{60}Co)	6	1.85 ± 0.05
2103.5 (^{208}Tl, $E_\gamma - m_o C^2$)	1	2.4 ± 0.2
2614.5 (^{208}Tl)	3	2.5 ± 0.1
6907	1	3.85 ± 0.1
7131	1	4.45 ± 0.1
8260	1	5.0 ± 0.1
9058	1	4.8 ± 0.1

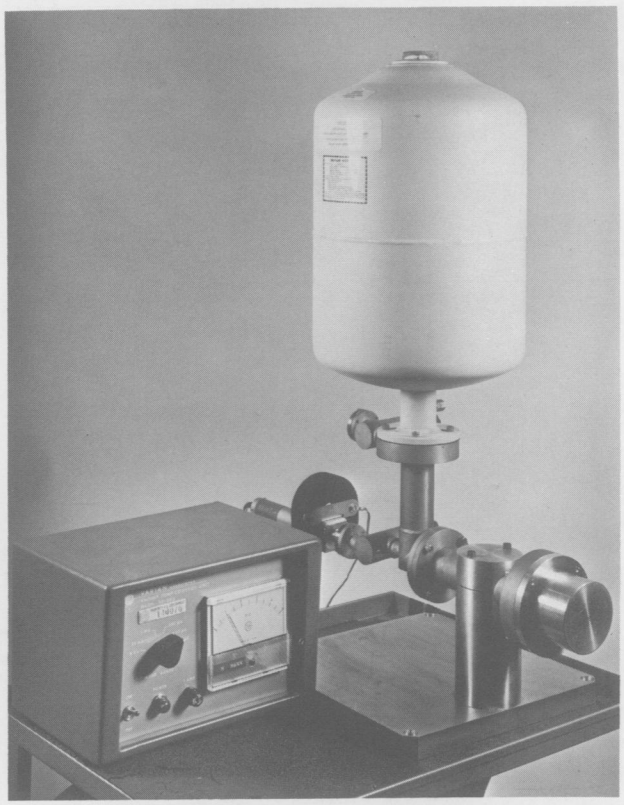

Fig. 1—Detector Chamber with liquid nitrogen storage reservoir.

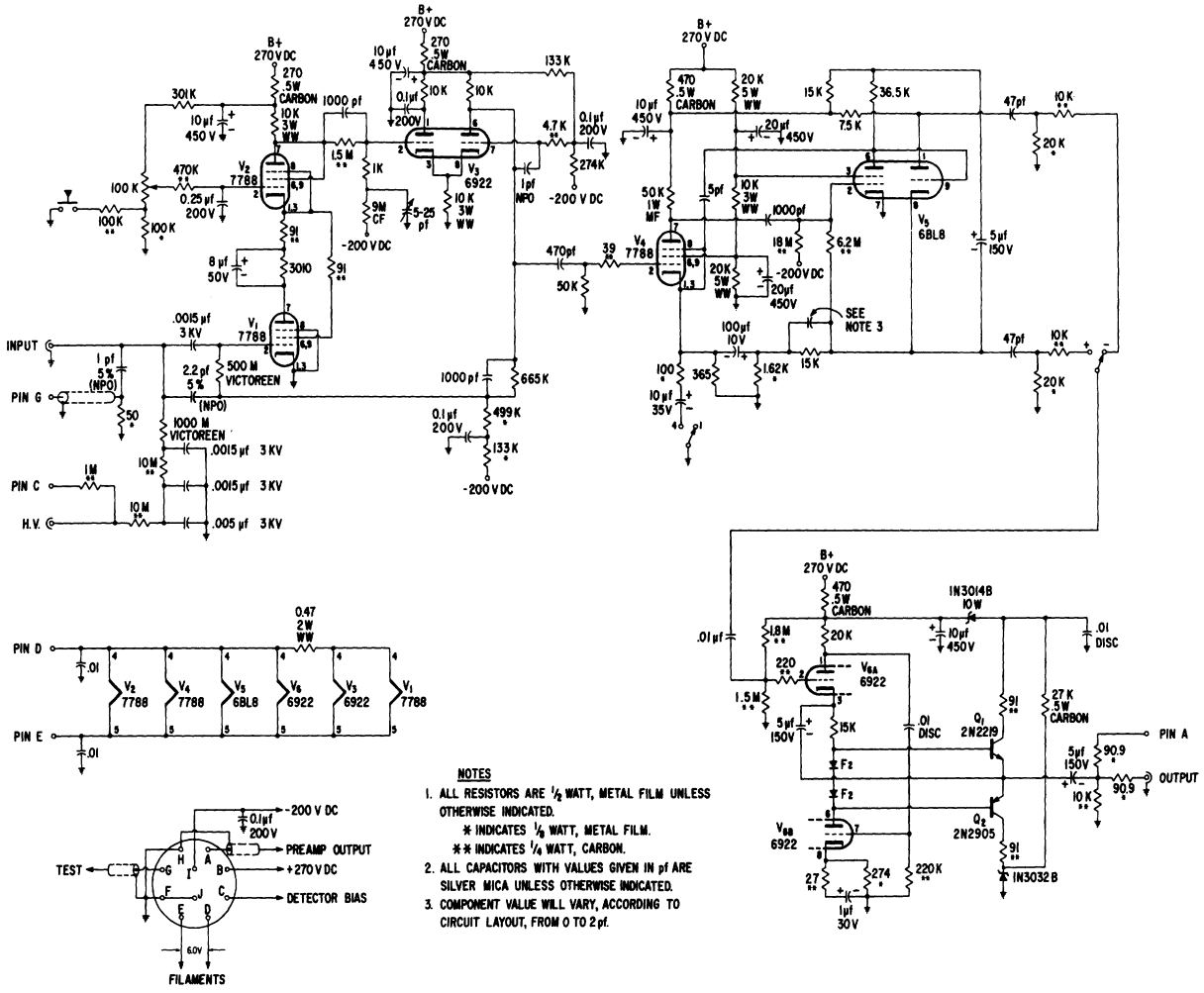

Fig. 2—Schematic diagram of low-noise vacuum tube preamplifier, Model PASD1.

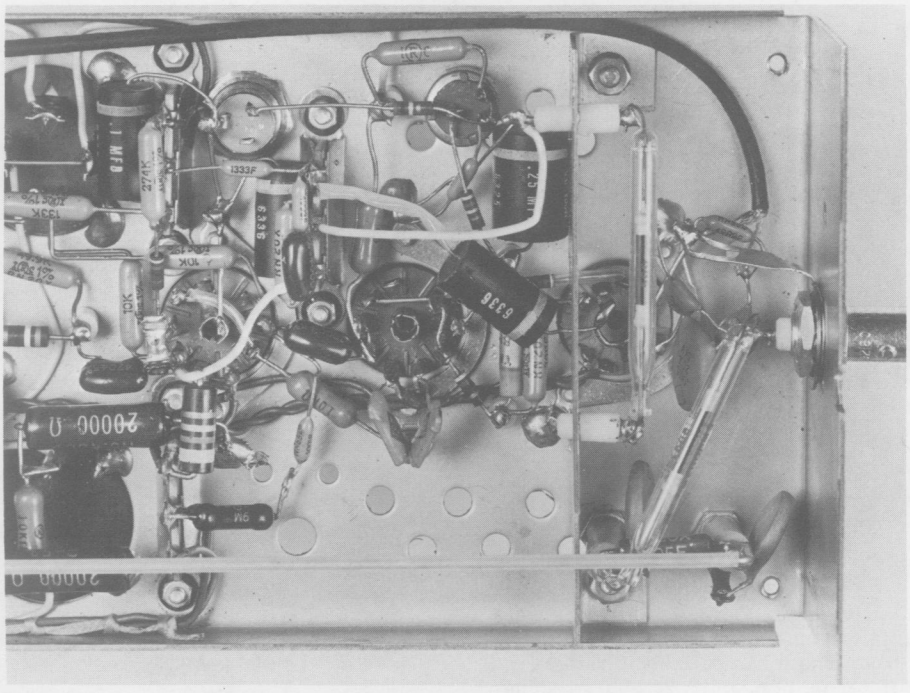

Fig. 3—Layout of input stage of Model PASD1 preamplifier.

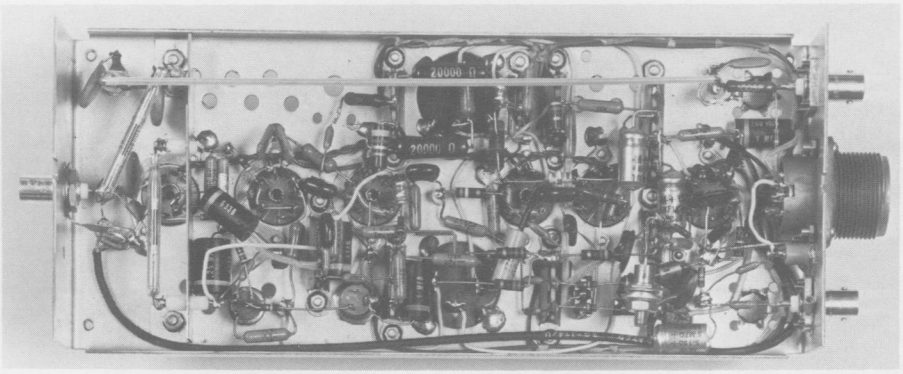

Fig. 4—Layout of components in Model PASD1 preamplifier.

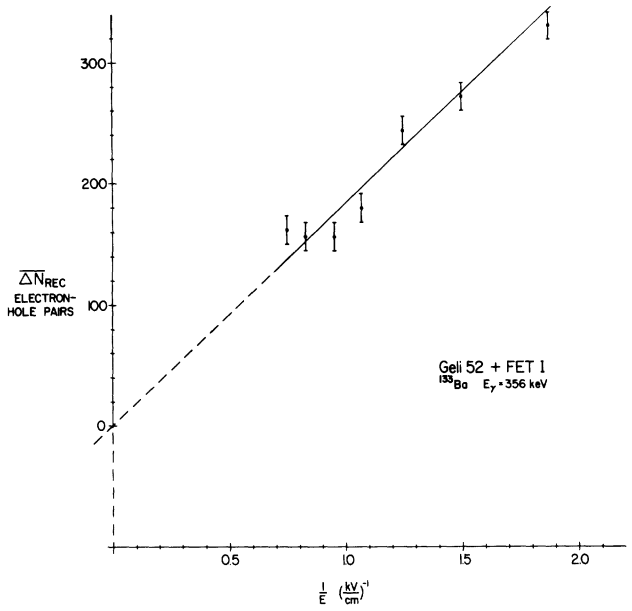

Fig. 5—Mean pulse height as a function of reciprocal electric field intensity for the 356 keV γ-rays from ^{133}Ba. The mean pulse height is expressed in terms of quantity of charge using ϵ = 2.8 eV per electron-hole pair.

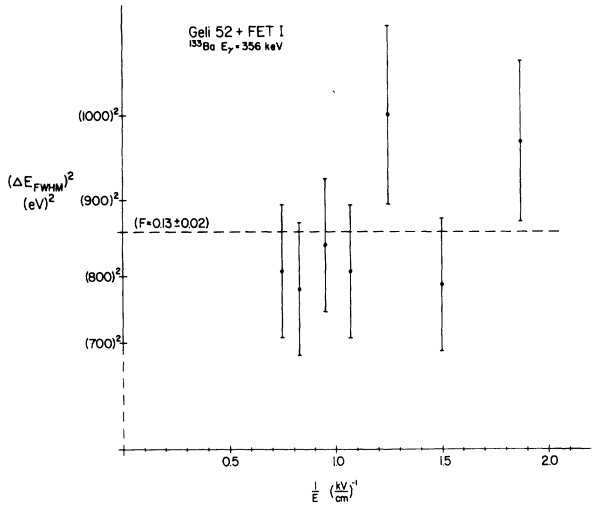

Fig. 6—Experimental data showing absence of a dependence of variance upon field intensity for the 356 keV γ-rays from ^{133}Ba.

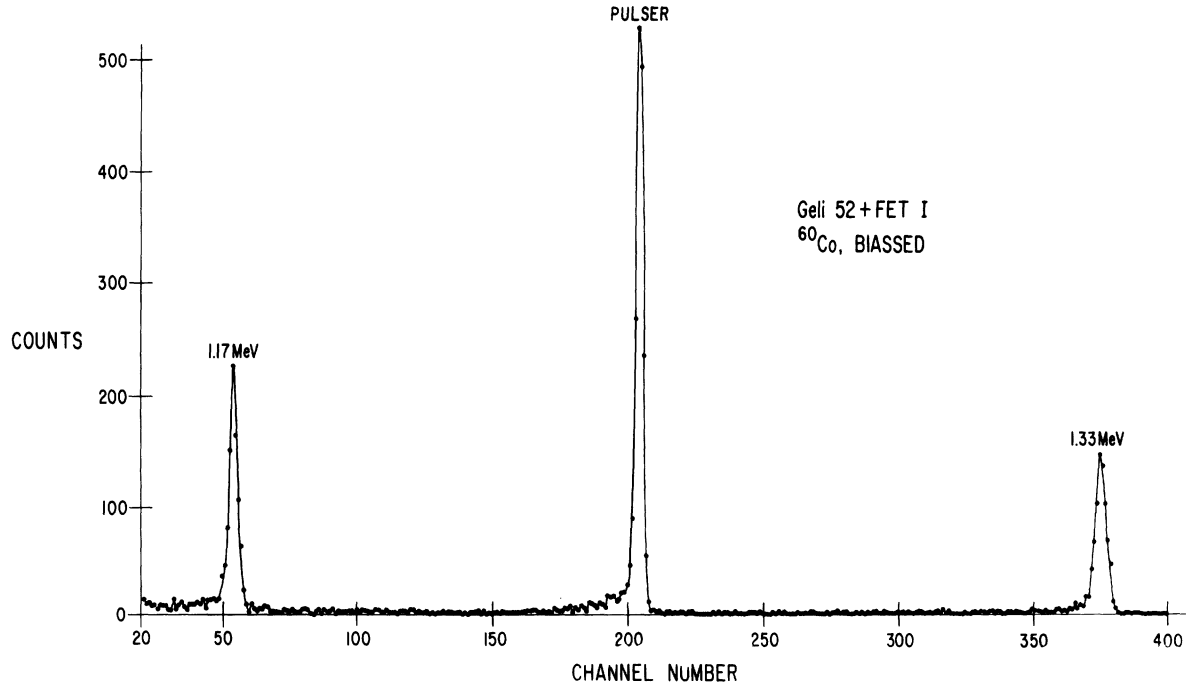

Fig. 7—Pulse height distribution for the 1.17 and 1.33 MeV γ-rays from ^{60}Co together with a pulser peak.

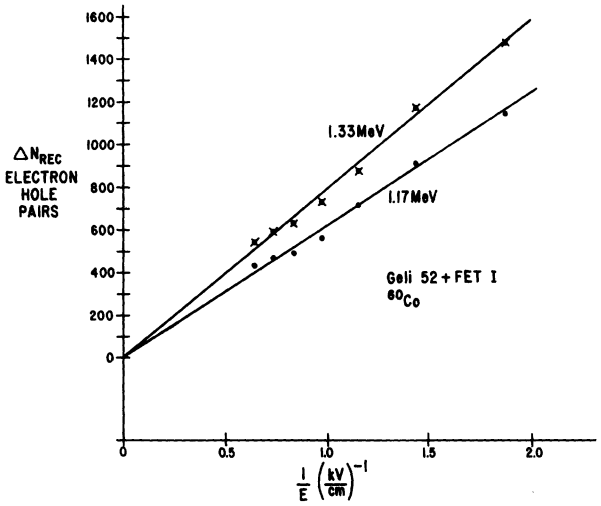

Fig. 8—Mean pulse height as a function of reciprocal electric field intensity for γ-rays from ^{60}Co. The mean pulse height is expressed in terms of quantity of charge using ϵ = 2.8 eV per electron-hole pair.

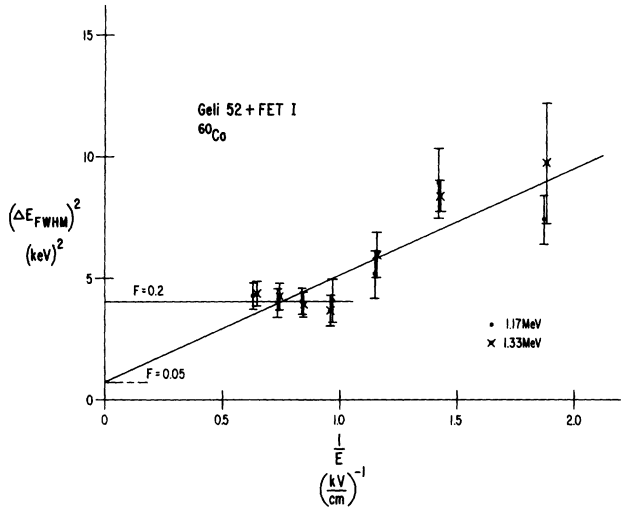

Fig. 9—Dependence of $\sigma^2/\bar{N}$ upon reciprocal electric field intensity for γ-rays of energy 1.17 and 1.33 MeV from ^{60}Co.

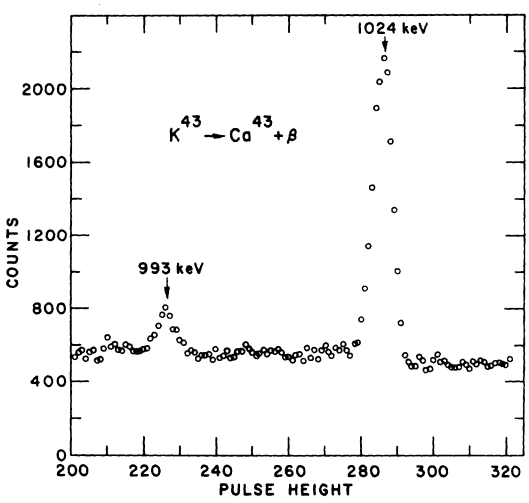

Fig. 10—Typical pulse height distribution for 993 and 1024 keV γ-rays observed in the decay of ^{43}K → ^{43}Ca + β.

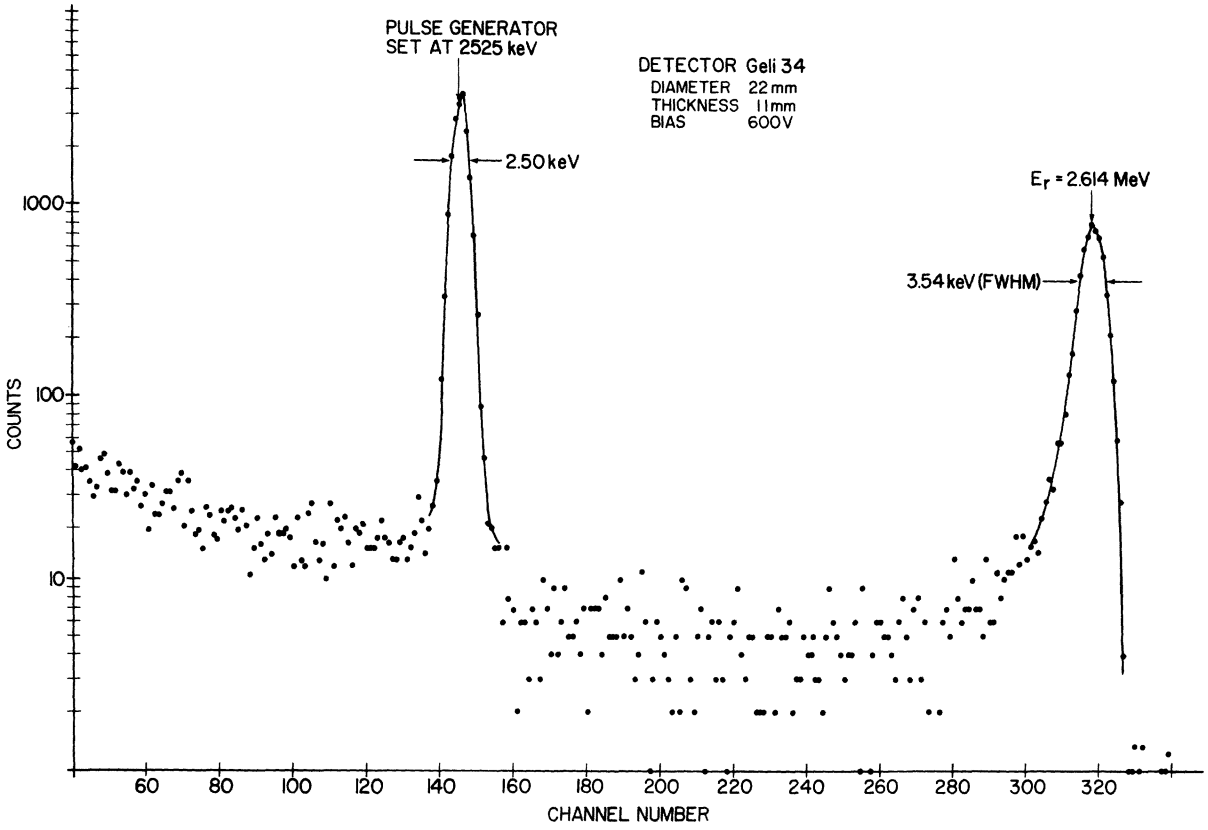

Fig. 11—Pulse height distribution for the 2614.5 keV γ-rays from ^{208}T1 together with a pulser peak. The amplitude of the pulse was preset to 2525 keV and the amplifier gain was then increased by a factor of 2.

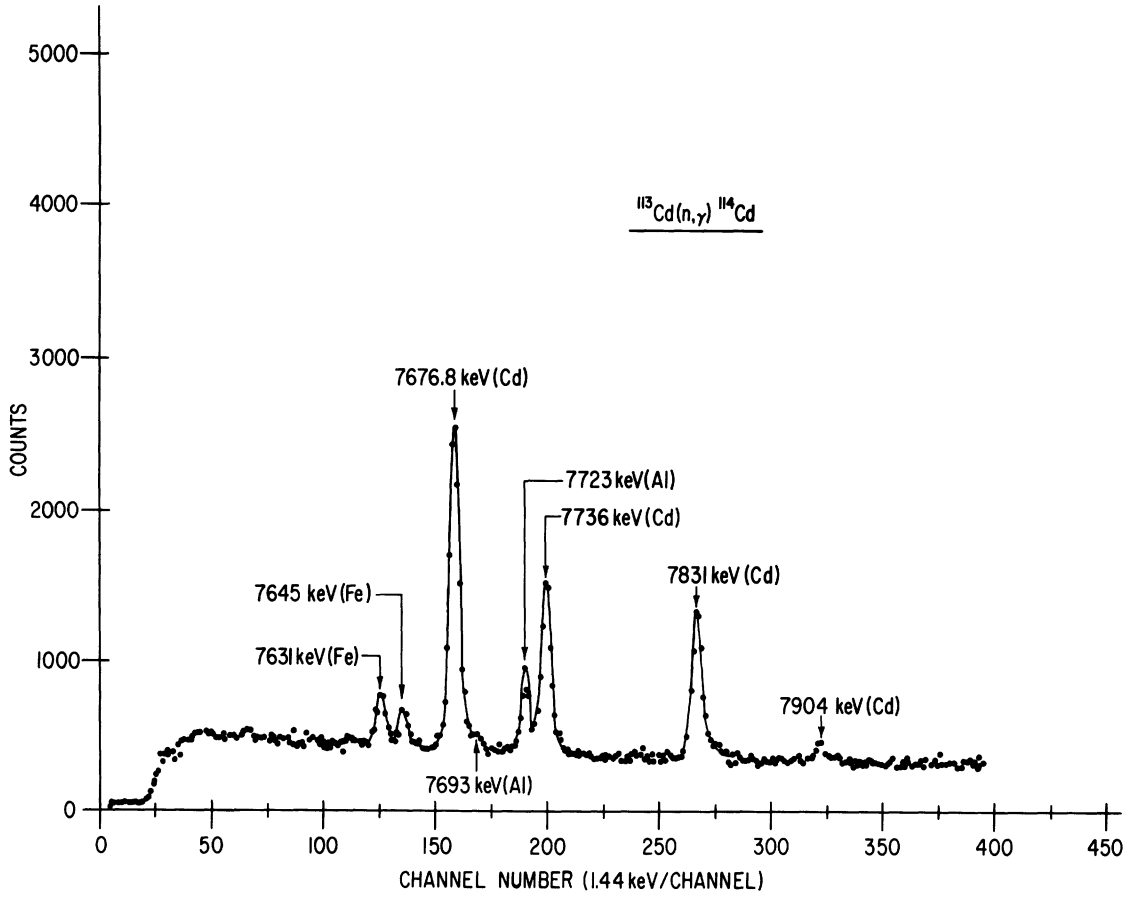

Fig. 12—Partial spectrum for γ-rays from the reaction ^{113}Cd (n, γ) ^{114}Cd as observed with a detector of thickness 11 mm and diameter 22 mm. The observed energy is reduced by 511 or 1022 keV by escape of annihilation radiation.

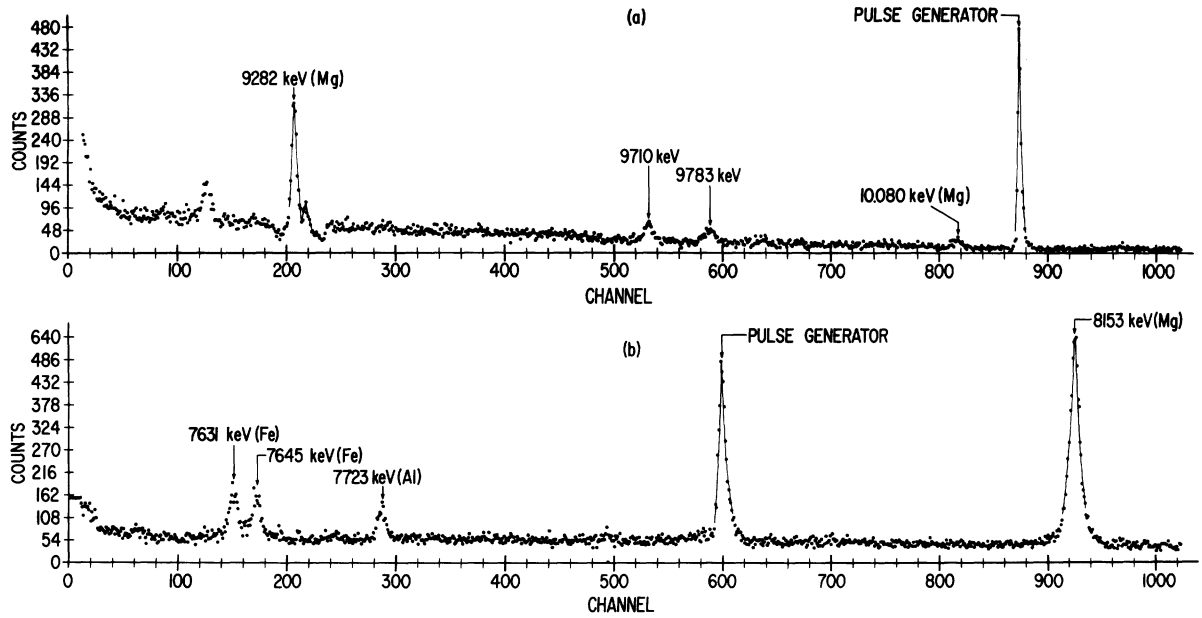

Fig. 13—Partial spectra for γ-rays from (n, γ) reactions in (a) Mg and (b) Fe and Al. The detector contribution to resolution width was determined for the various energy values shown. The observed energy is reduced by 511 or 1022 keV by escape of annihilation radiation.

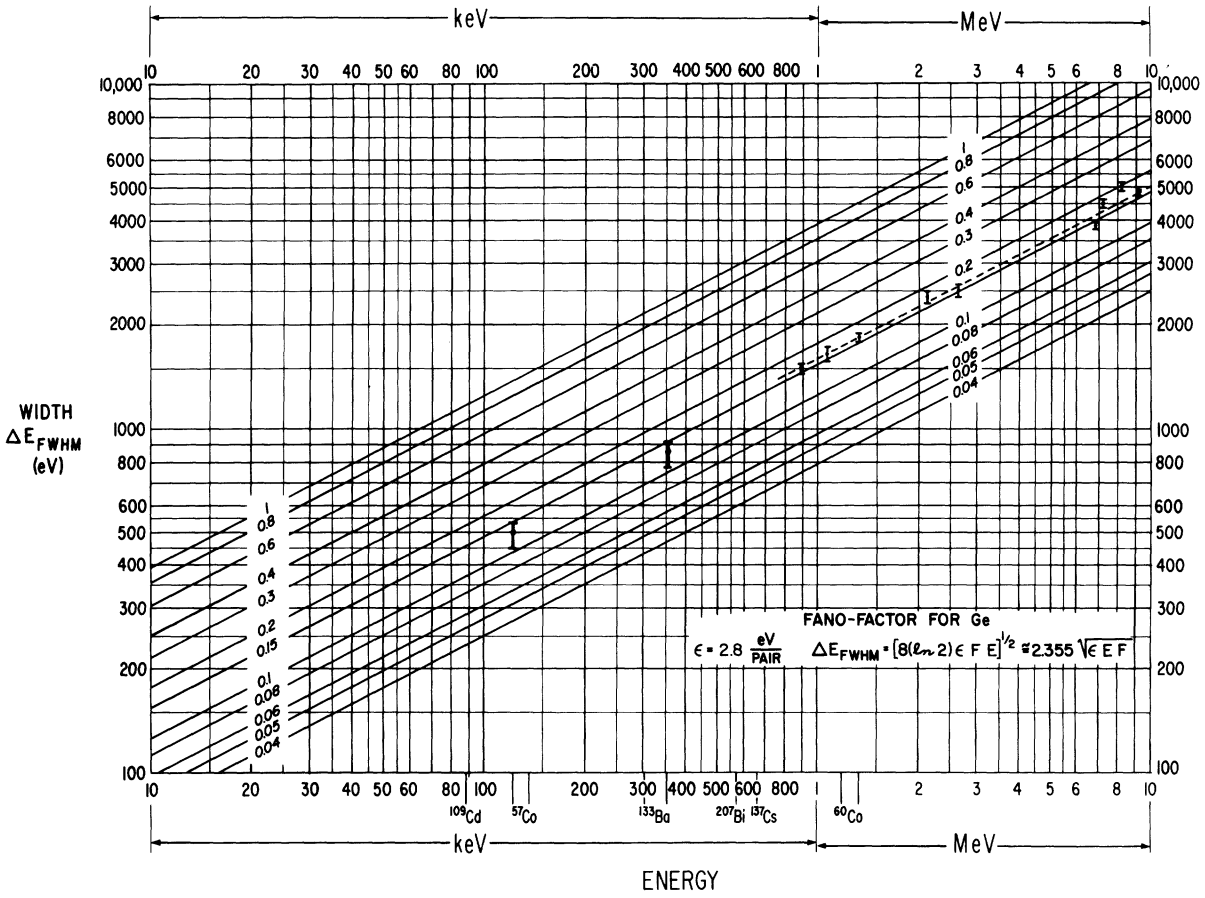

Fig. 14—Resolution width as a function of energy, parametric in Fano factor, for germanium detectors. The results of measurements at various energies are shown.

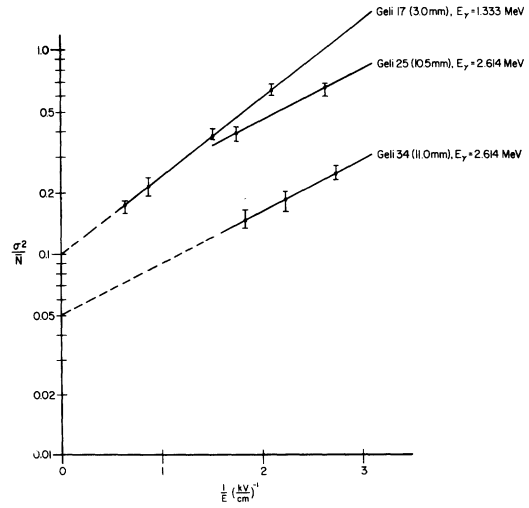

Fig. 15—Dependence of $\sigma^2/\bar{N}$ upon reciprocal electric field intensity for several detectors.